New and Corrected Simulations of Synaptic Facilitation

Victor Matveev,* Arthur Sherman,* and Robert S. Zucker†

*Mathematical Research Branch, National Institute of Diabetes and Digestive Kidney Diseases, National Institutes of Health, Bethesda, Maryland 20892 and †Molecular and Cell Biology Department, Neurobiology Division, University of California, Berkeley, California 94720 USA

Tang et al. (2000) demonstrated that, at the crayfish neuromuscular junction, both the accumulation and the decay properties of short-term synaptic facilitation (STF) are strongly affected by the addition of a fast high-affinity Ca^{2+} buffer, suggesting a role of residual free Ca^{2+} in the induction of STF. The authors proposed that the experimental results can be explained by a secretion model with two Ca^{2+} binding sites, a secretory site mediating exocytosis and located close to the Ca^{2+} channel (~10–20 nm), and a high-affinity facilitation site located further away (~80–100 nm) from the channel. Here we report that the data presented in Figs. 3, *C* and *D*, 6, and 7 of the original article, showing numerical solutions to the Ca^{2+} diffusion equations, are qualitatively inaccurate, because of misstated parameter values and, to a lesser extent, numerical algorithm errors. Therefore, some of the conclusions stated by Tang et al. concerning the proposed model require reexamination. In this letter we show that most of the predictions of the model hold, after an appropriate change of parameter values. Namely, the model correctly predicts the magnitude of STF, and the reduction of STF magnitude and acceleration of its decay in the presence of a fast high-affinity exogenous Ca^{2+} buffer, such as Fura-2. The fast ("F1") and slow ("F2") decay components of STF are also successfully reproduced, if an additional assumption is made that the endogenous Ca^{2+} buffers are immobile. However, our simulations predict that the slower F2 decay component is completely abolished in the presence of Fura-2, contrary to experimental results of Tang et al. (2000) (Fig. 3, *A* and *B*, in the original paper). We found that this remaining disagreement can be resolved if one assumes that the diffusion in the synaptic bouton is restricted, so that 1) in a 200-nm layer around the active zone, Fura-2 is immobilized and the diffusion coefficient of Ca^{2+} is reduced fivefold, due to a high degree of tortuosity; and 2) in the rest of the terminal, the diffusion coefficient of Fura-2 is reduced 100-fold (presumably because of binding to various cytosolic compounds). Moreover, contrary to the statement by Tang et al. that their model fails to accurately describe the accumulation time course of STF, we show that the model modifications that we propose lead to a supralinear growth of STF, in agreement with experiment (Fig. 2, *A* and *D*).

Submitted February 22, 2002, and accepted for publication May 7, 2002.

Address reprint requests to Victor Matveev, 9190 Rockville Pike, Suite 350, Bethesda, MD 20892. Tel.: 301-496-9644; Fax: 301-402-0535; E-mail: matveev@nih.gov.

0006-3495/02/09/1368/06 $2.00

Facilitation magnitude: role of fixed buffers in STF

An attempt to reproduce the simulation results presented in Figs. 3, *C* and *D*, 6, and 7 of Tang et al., 2000, using a newly developed computer program, CalC (see below), revealed significant discrepancies. To resolve this disagreement, we analyzed the computer code used to generate Ca^{2+} traces in Fig. 7 *B* of the original article (developed by Thomas Schlumpberger), and found that the parameter values used in the simulations were different from the values quoted in the paper. The differences between the two parameter sets are summarized in Table 1. Fig. 1 demonstrates the difference in $[Ca^{2+}]$ profiles at the STF site computed using the *quoted* and *actual* parameter values (*thick* and *thin* lines, respectively), and compares them to the original Fig. 7 *B* of Tang et al. (*dashed line*). One can see that, even when using the same parameter values, there remains a significant quantitative disagreement between our simulations and the original figure (compare the *dashed* and *thick curves* in Fig. 1). We found that this remaining discrepancy is a result of an algorithm error in the original code, in the realization of the elementary compartment size doubling (see subsection "Implementing differential equations" of the Materials and Methods section of Tang et al., 2000, page 2736).

In a model with a fast STF site (included to account for rapid reduction of STF by photolabile Ca^{2+} buffers; Kamiya and Zucker, 1994), the magnitude of STF is determined by the size of residual $[Ca^{2+}]$ relative to the peak $[Ca^{2+}]$ achieved during an AP. Fig. 1 shows that, for the *quoted* parameter values, Ca^{2+} concentration at the STF site is characterized by large transients, which are significantly greater than the residual $[Ca^{2+}]$, resulting in small facilitation magnitude (numerical result not shown). STF magnitude computed using the *actual* parameters, although still below the experimental value (compare Fig. 2, *A* and *B*), is significantly larger. Our simulations show that the critical parameters responsible for this difference are the total concentration and the Ca^{2+} binding rate of the fixed buffer, both of which are higher for the *actual* parameter set. The fixed buffer is critical in maintaining large STF: unlike mobile buffers, which carry Ca^{2+} away from the synaptic

TABLE 1 Discrepancy between the quoted and the actual parameter values

Parameter	Quoted value	Actual value
Ca^{2+} diffusion coefficient	223 $\mu m^2/s$	200 $\mu m^2/s$
Mobile buffer diffusion coefficient	50 $\mu m^2/s$	10 $\mu m^2/s$
Mobile buffer total concentration	280 μM	560 μM
Mobile buffer binding rate (k_{on})	0.1 $\mu M^{-1}\,ms^{-1}$	0.5 $\mu M^{-1}\,ms^{-1}$
Mobile buffer unbinding rate (k_{off})	0.2 ms^{-1}	2 ms^{-1}
Mobile buffer affinity ($K_D=k_{off}/k_{on}$)	2 μM	4 μM
Fixed buffer total concentration	5.76 mM	8 mM
Fixed buffer binding rate (k_{on})	0.1 $\mu M^{-1}\,ms^{-1}$	0.5 $\mu M^{-1}\,ms^{-1}$
Fixed buffer unbinding rate (k_{off})	1.6 ms^{-1}	8 ms^{-1}
Fixed buffer affinity ($K_D = k_{off}/k_{on}$)	16 μM	16 μM
Ca^{2+} current	1.35×10^{-18} mol/s	1.08×10^{-18} mol/s
Ca^{2+} tail current	4.6×10^{-18} mol/s	3.68×10^{-18} mol/s
Distance between nearest channels	40 nm	60 nm
Distance from facilitation site to channel	100 nm	70 nm
Ca^{2+} pumps	on two surfaces	on one surface only

A comparison between values used to generate Fig. 7 *B* of Tang et al., 2000 (*actual values*) and the values quoted on pp. 2741 and 2742 of that paper (*quoted values*). The *actual* parameter set is characterized by smaller current strength and channel density (greater distance between channels), higher concentration of the fixed buffer, lower affinity and mobility of the diffusible buffer, and higher Ca^{2+} binding rate of both endogenous buffers.

terminal, decreasing residual $[Ca^{2+}]$ and thereby reducing the STF (unless they are saturated; see below), fixed buffers prevent Ca^{2+} from diffusing away. This slows down the Ca^{2+} signal and prolongs its action near the secretory and facilitation machinery, which in turn leads to greater STF (Sala and Hernández-Cruz, 1990; Nowycky and Pinter, 1993; Neher, 1998; Kits et al., 1999). We note that this mechanism is distinct from the buffer saturation mechanism put forward by E. Neher (Neher, 1998; Rozov et al., 2001) as a potential source of STF. In the latter situation, the increase in response results from the increase in Ca^{2+} transients, caused by reduced buffering capacity associated with buffer saturation, whereas in our simulations the response growth is caused predominantly by the increase in residual $[Ca^{2+}]$.

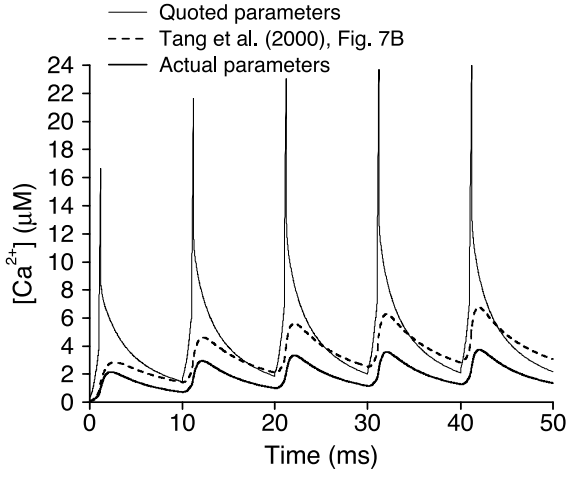

FIGURE 1 Ca^{2+} concentration at the facilitation site, in response to a 5-pulse stimulation train. *Thin line:* simulation results for parameter values quoted in Tang et al., 2000; *thick line:* simulation results for the parameter set used to generate Fig. 7 *B* of Tang et al., 2000 (see Table 1); *dashed line:* the control (100% external Ca^{2+}) curve from Fig. 7 *B* of Tang et al., 2000. The discrepancy between the thick and dashed lines is due to the algorithm errors in the original work.

STF decay time course: excluding mobile buffers

The main disagreement between our results and the simulation results reported in the original paper concerns the decay time course of STF: although Fig. 3, *C* and *D*, of Tang et al. reveals both the F1 and F2 decay components of STF, we were not able to reproduce the slower F2 component, neither using the *quoted* parameter values (data not shown; STF is very small in this case), nor the *actual* values (in the latter case, STF decayed with time constants of 5 ms and 21 ms; see Fig. 3 *B* and Table 2). This is to be expected, because the time scales of Ca^{2+} processes implemented in the model are either much faster (Ca^{2+} unbinding from buffers, Ca^{2+} unbinding from the STF sensor, buffered diffusion of Ca^{2+}) or much slower (Ca^{2+} extrusion by membrane pumps) than the time scale of hundreds of milliseconds characterizing the F2 decay component. The only way to prolong STF decay within the framework of the current model is to slow the buffered diffusion of calcium by assuming that the endogenous Ca^{2+} buffers are predominantly present in *fixed* form. To this end, we repeated our simulations with a new ("modified") parameter set, which is similar to the *actual* parameter set in Table 1, with the exception that the mobile buffer is excluded. Furthermore, we placed the secretory site 10 nm away, and the STF site at a distance of 100 nm away from the nearest Ca^{2+} channel. Simulations with this *modified* set of parameters revealed higher STF magnitude (Fig. 2 *C*), in better

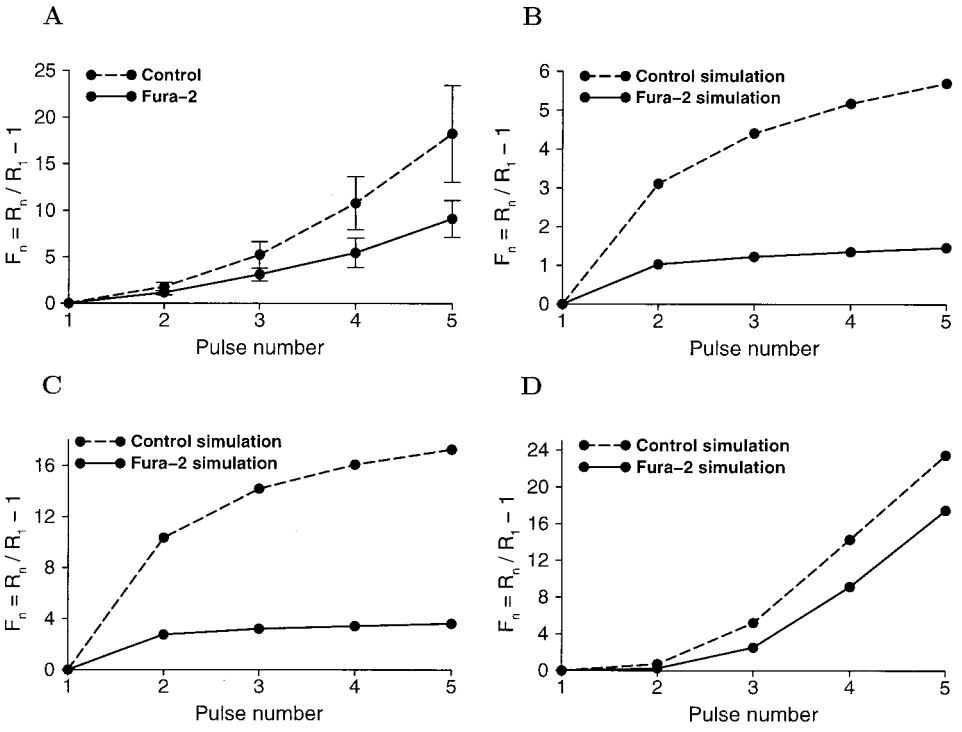

FIGURE 2 Accumulation time course of synaptic facilitation elicited by a 5-pulse train, with and without the addition of Fura-2. (*A*) Experimentally measured facilitation, from Tang et al., 2000, Fig. 2 *C* (*control* curve, 100% external Ca^{2+}). (*B*) Simulation results for the *actual* parameter set from Table 1. (*C*) Simulation without mobile buffer (*modified* parameter set: see text): notice higher STF magnitude. (*D*) Simulation without mobile buffer, with tortuosity effects included (see text); notice the supralinear shape of the curve, similar to *A*. In *B* and *C*, Ca^{2+} binding scheme and Fura-2 properties (affinity = 360 nM, D_{F2} = 118 $\mu m^2/s$, $[Fura\text{-}2]_{total}$ = 400 μM, unbinding rate = 96.7 s^{-1}) are the same as in Tang et al., 2000. In *D*, the Ca^{2+} affinity of the STF site was changed from 3 to 9 μM; Fura-2 is immobile in a 200-nm layer around the active zone; in the rest of the terminal D_{F2} = 1.18 $\mu m^2/s$.

agreement with experiment (Fig. 2 *A*), and a slower STF decay (Fig. 3 *C*), with F1 and F2 decay time constants of 28 ms and 135.5 ms, respectively (Table 2). However, as soon as Fura-2 is included in the model, the F2 component isn't just reduced and accelerated, as seen experimentally (Fig. 3 *A*), but is completely removed (Fig. 3 *C*; Table 2). This agrees with our earlier remarks about the opposing actions of mobile and fixed buffers on STF. We were not able to obtain the F2 component with Fura-2 present without additional modifications to the model; we believe that the results in the original Fig. 3, *C* and *D* of Tang et al. are due to an algorithm or implementation error that we have not been able to identify.

STF decay with Fura-2: implementing tortuosity

To retain the slow decay component of STF in the presence of Fura-2, we have to assume that some additional mechanisms are impeding diffusion in the synaptic bouton. To test this possibility, we incorporated tortuosity into the model by reducing the diffusion coefficients of both Fura-2 and Ca^{2+} in a 200-nm-wide layer around the active zone, assuming that diffusion is obstructed in this region by vesicles and various synaptic proteins. As an alternative, we investigated the effect of slowing the diffusion of Fura-2 alone in the entire volume, simulating the effects of Fura-2 binding to various cytosolic compounds (such an effect has been observed in muscle cells by Konishi et al., 1988 and Baylor and Hollingworth, 1988; see also Kits et al., 1999). We found that either condition by itself is not sufficient to achieve the desired behavior (see, respectively, Table 2, *Simulations with tortuosity*, row *Fura-2*, and *Modified parameter set*, row *slow Fura-2*), and that both effects have to be included to account for experimental results. The best agreement with experiment was achieved with the following changes to the *modified* parameter set defined earlier: 1) in a 200-nm layer around the active zone, Fura-2 is immobilized and the diffusion coefficient of Ca^{2+} is reduced fivefold; 2) in the rest of the terminal, the diffusion coefficient of Fura-2 is reduced 100-fold; 3) the facilitation site is moved to 180 nm away from the plasma membrane; and 4) the Ca^{2+} affinity of the STF site is changed from 3 μM to 9 μM.

The corresponding results are shown in Figs. 2 *D* and 3 *D*; the decay components are given in Table 2, *Simulations with tortuosity*, row *slower Fura-2*. In an attempt to use the most realistic parameters, in these simulations we also reduced the on-rate of the fixed buffer to 0.05 μM^{-1} ms^{-1}

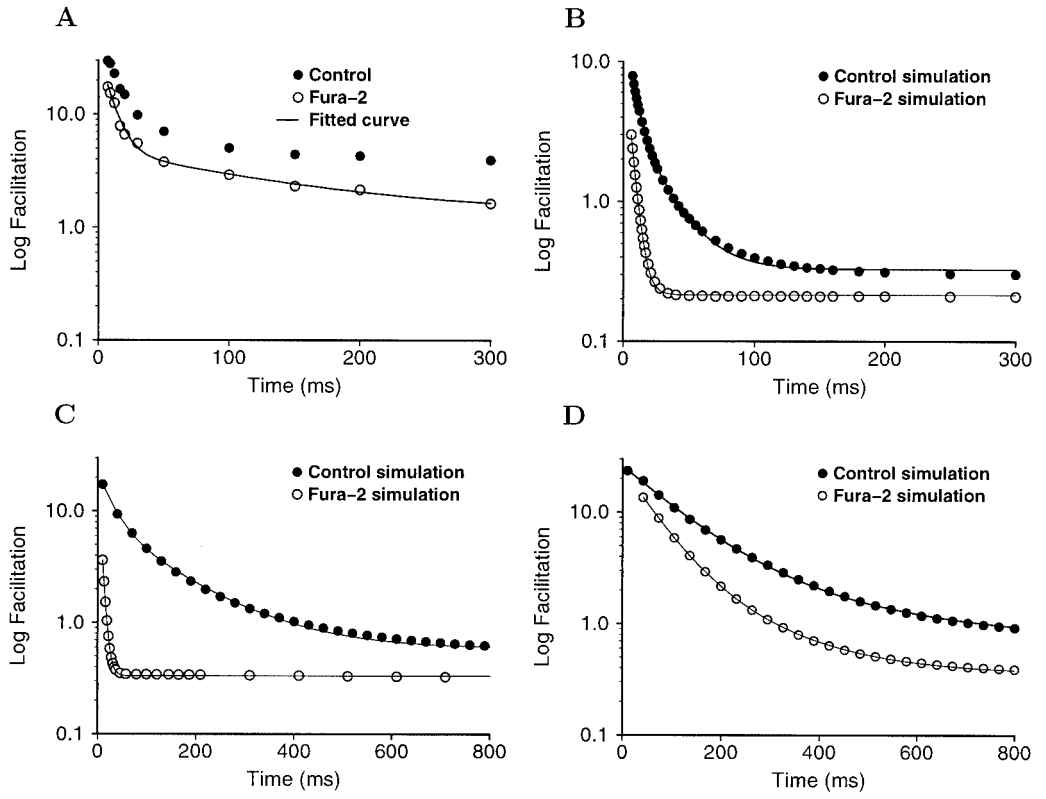

FIGURE 3 Decay time course of synaptic facilitation elicited by a 5-pulse train, as a function of time interval between the 4th and 5th pulses, with and without the addition of Fura-2. (*A*) Experimentally measured facilitation, from Tang et al., 2000, Fig. 3 *B*. (*B*) Simulation results for the *actual* set of parameters from Table 1. (*C*) Simulation without mobile buffer ("modified" parameter set: see text). (*D*) Simulation without mobile buffer, with tortuosity effects included. Continuous curves drawn through the data points correspond to exponential fits to the simulation results; the corresponding time constants and amplitudes are listed in Table 2 (for *C* and *D*, the corresponding entries are shown in boldface). Parameters are the same as in Fig. 2.

and the off-rate to 0.8 ms^{-1}. This additional change had only a negligible effect on results. Note that the *quoted* fixed buffer rate constants of Tang et al. (2000) are slower than the *actual* rate constants. The *quoted* values were based on measurements of Xu et al. (1997) for buffer on-rates in bovine chromaffin cells. The ionic strength of crayfish cytoplasm is twice that of vertebrates, and so the on-rate is likely to be even slower, probably 0.05 μM^{-1} ms^{-1}. To retain the measured buffer ratio of ~500 (Delaney and Tank, 1994), we leave K_D at 16 μM and total buffer concentration at 8 mM, and reduce the off-rate to 0.8 ms^{-1}.

There is an additional reason to use slower buffer kinetics. Flash photolysis of the photolabile calcium chelator DM-nitrophen produces a rapid phase of transmitter release that reflects the presence of a "calcium spike," caused by the rapid release of calcium and its slower (2 ms) rebinding to the unphotolyzed DM-nitrophen (Landò and Zucker, 1994). Simulations of the effects of the native buffer on the "calcium spike," using recently described kinetic constants for DM-nitrophen binding to magnesium, which is responsible for the slow rebinding of calcium (Ayer and Zucker, 1999), show that a buffer on-rate of 0.05 μM^{-1} ms^{-1} is most consistent with the experimental results of Landò and Zucker (1994) (R. S. Zucker, unpublished observations).

Supralinear growth of STF

In the original article, the authors stated that their model failed to reproduce the experimentally observed accumulation time course of STF (compare Fig. 2, *A* and *B*). However, our results in Fig. 2 *D* show that the changes listed above, apart from explaining the decay behavior of STF, also enable the model to successfully reproduce the supralinear growth of STF. We found that tortuosity is not necessary for this effect, and that supralinear growth of STF can also be achieved with the *modified* parameter set, if the distance between the STF site and Ca^{2+} channel is >250 nm (simulations not shown). We found that the presence of fixed Ca^{2+} buffers is crucial for this property. The reason for this is that the fixed buffer effectively adds intermediate Ca^{2+} binding stages to the facilitation process, because the Ca^{2+} ions would have to undergo multiple buffer binding and unbinding steps on their way to the STF site. It has been noted previously by Balnave and Gage (1977) that adding

TABLE 2 The amplitudes and time constants of the two components of the STF decay

		F1	τ_1 (ms)	F2	τ_2 (ms)
Experiment	Control	21.8 ± 12.5	18.6 ± 4.9	4.1 ± 1.2	536 ± 222
(Tang et al., 2000)	Fura-2	16.1 ± 8.9	12.2 ± 3.3	2.4 ± 1.0	365 ± 222
Actual parameter set	Control	17.4, 4.3	5.1, 21.6	n/a	n/a
	Fura-2	11.6	4.2	n/a	n/a
Modified parameter set	**Control**	**13.9**	**28.1**	**7.4**	**135.5**
	Fura-2	**18.1**	**5.9**	**n/a**	**n/a**
	Slow Fura-2	16.8	25.7	5.8	89
Simulations with tortuosity	**Control**	**22.3**	**106.5**	**2.91**	**335**
	Fura-2	1.0	13.3	n/a	n/a
	Slow Fura-2	17.6	61	7.3	133
	Slower Fura-2	**20.8**	**60.5**	**3.56**	**162**

For the *actual* parameter set, two decay components in the control (no Fura-2) simulation are listed in the F1 column, because both are very fast. The diffusion coefficient of Fura-2 is set to $D_{F2} = 118\ \mu m^2/s$ except for the following entries: *Modified parameter set, slow Fura-2*: $D_{F2} = 0.69\ \mu m^2/s$; note that in this case there is no reduction of STF by Fura-2 for short inter-pulse intervals, given by the sum of the F1 and F2 amplitudes; *simulations with tortuosity, slow Fura-2*: $D_{F2} = 0.69\ \mu m^2/s$. In the 200-nm-wide layer around the active zone, diffusion coefficients of both Fura-2 and Ca^{2+} are reduced fivefold; *slower Fura-2*: Fura-2 is immobile (and the diffusion coefficient of Ca^{2+} is reduced fivefold) in the 200-nm-wide layer around the active zone; in the rest of the terminal $D_{F2} = 1.18\ \mu m^2/s$. Boldface entries correspond to Fig. 2, *C* and *D*, and Fig. 3, *C* and *D*. We note that the fit results are highly sensitive to the minimal value, Δt_{min}, of the inter-pulse interval between the control and test pulses. $\Delta t_{min} = 10$ ms in all simulations except for the Fura-2 simulations with tortuosity (cells *slow Fura-2* and *slower Fura-2*), where a value $\Delta t_{min} = 41$ ms is used, because the decay of STF for small inter-pulse intervals is not exponential (see Fig. 3 *D*).

intermediate Ca^{2+} binding steps to a facilitation model is sufficient to reproduce the supralinear STF growth. In general, increasing the number of steps in a kinetic process makes its transient behavior progressively more supralinear in time. Tortuosity potentiates this effect by increasing the effective time it takes a Ca^{2+} ion to diffuse to the STF site, so the supralinearity can be achieved for smaller separations between the STF site and the Ca^{2+} channel. This is desirable because the STF site is likely to be located close to the release machinery, where it can have an immediate effect on the release process. Therefore, including tortuosity allows the model to explain the supralinear growth of STF for more physiologically realistic distances between the STF site and the Ca^{2+} channel.

CONCLUSION

For a suitable choice of parameters, and assuming that endogenous Ca^{2+} buffers are present predominantly in fixed form, the model proposed by Tang et al. (2000) agrees with the observed accumulation and decay properties of STF at the crayfish neuromuscular junction, but predicts stronger reduction of STF by fast high-affinity exogenous Ca^{2+} buffers than seen experimentally. To explain the properties of STF in the presence of Fura-2, we have to impose an additional assumption that the diffusion in the vicinity of the active zone is significantly retarded due to tortuosity effects, and that Fura-2 is also strongly slowed in the rest of the terminal. We also moved the facilitation site to 180 nm from the nearest Ca^{2+} channel. Given the highly constricted space surrounding a docked vesicle, filled with a variety of proteins and cytoskeletal elements, a diffusion distance of 180 nm is not only within the active zone, but may well be within the complex of proteins involved with vesicle exocytosis (Tang et al., 2000). In addition, we decreased the affinity of the facilitation site to 9 μM, less than the affinity of a high-affinity site estimated by Ravin et al. (1997) but consistent with the observations of Delaney and Tank (1994). With these modifications the model also reproduces the experimentally observed supralinear growth of STF. Our analysis of the model reveals that the fixed endogenous Ca^{2+} buffers play a crucial role in the STF process.

Numerical simulations

All new numerical results presented here were performed using the CalC (Calcium Calculator) computer software, freely available from the URL (http://mrb.niddk.nih.gov/matveev). CalC currently runs on Linux, SGI, and Windows/Intel platforms, and is driven by a user-friendly script. We ensured that our program is error-free by checking it against simple, exactly solvable problems, and by reproducing some of the modeling results found in the literature. Furthermore, we verified that our results agreed with the output of the original code in the absence of the compartment size doubling. We also checked the convergence of results when spatial and temporal resolutions were increased. Simulation parameters were chosen to maintain a numerical accuracy of ~5%. To render the results reported here easily reproducible, and to provide a detailed description of the simulations, the corresponding commented script files will be made available at the web site given above.

We thank Dr. Jim Winslow for careful reading of this manuscript. This work was supported in part by National Institutes of Health Grant NS15114 (to R.S.Z.).

REFERENCES

Ayer, R. K., Jr., and R. S. Zucker. 1999. Magnesium binding to DM-nitrophen and its effect on the photorelease of calcium. *Biophys. J.* 77:3384–3393.

Balnave, R. J., and P. W. Gage. 1977. Facilitation of transmitter secretion from toad motor nerve terminals during brief trains of action potentials. *J. Physiol.* 266:435–451.

Baylor, S. M., and S. Hollingworth. 1988. Fura-2 calcium transients in frog skeletal muscle fibres. *J. Physiol.* 403:151–192.

Delaney, K. R., and D. W. Tank. 1994. A quantitative measurement of the dependence of short-term synaptic enhancement on presynaptic residual calcium. *J. Neurosci.* 14:5885–5902.

Kamiya, H., and R. S. Zucker. 1994. Residual calcium and short-term synaptic plasticity. *Nature.* 371:603–606.

Kits, K. S., T. A. de Vlieger, B. W. Kooi, and H. D. Mansvelder. 1999. Diffusion barriers limit the effect of mobile calcium buffers on exocytosis of large dense cored vesicles. *Biophys. J.* 76:1693–1705.

Konishi, M., A. Olson, S. Hollingworth, and S. M. Baylor. 1988. Myoplasmic binding of fura-2 investigated by steady-state fluorescence and absorbance measurements. *Biophys. J.* 54:1089–1104.

Landò, L., and R. S. Zucker. 1994. Ca^{2+} cooperativity in neurosecretion measured using photolabile Ca^{2+} chelators. *J. Neurophysiol.* 72: 825–830.

Neher, E. 1998. Usefulness and limitations of linear approximations to the understanding of Ca^{++} signals. *Cell Calcium.* 24:345–357.

Nowycky, M. C., and M. J. Pinter. 1993. Time courses of calcium and calcium-bound buffers following calcium influx in a model cell. *Biophys. J.* 64:77–91.

Ravin, R., M. E. Spira, H. Parnas, and I. Parnas. 1997. Simultaneous measurement of intracellular Ca^{2+} and asynchronous transmitter release from the same crayfish bouton. *J. Physiol.* 501:251–262.

Rozov, A., N. Burnashev, B. Sakmann, and E. Neher. 2001. Transmitter release modulation by intracellular Ca^{2+} buffers in facilitating and depressing nerve terminals of pyramidal cells in layer 2/3 of the rat neocortex indicates a target cell-specific difference in presynaptic calcium dynamics. *J. Physiol.* 531:807–826.

Sala, F., and A. Hernández-Cruz. 1990. Calcium diffusion modeling in a spherical neuron. Relevance of buffering properties. *Biophys. J.* 57: 313–324.

Schlumpberger, T. 1999. Computational modeling of calcium action in synaptic facilitation. Ph.D. Dissertation, University of California, Berkeley, California.

Xu, T., M. Naraghi, H. Kang, and E. Neher. 1997. Kinetic studies of Ca^{2+} binding and Ca^{2+} clearance in the cytosol of adrenal chromaffin cells. *Biophys. J.* 73:532–545.